BMB Reports - Manuscript Submission

Manuscript Draft

Manuscript Number: BMB-16-220

Title: Heme oxygenase-1 (HO-1)/carbon monoxide (CO) axis suppresses RANKL-induced osteoclastic differentiation by inhibiting redox-sensitive NF-κB activation

Article Type: Article

Keywords: RANKL; osteoclastogenesis; HO-1/CO; NF-κB

Corresponding Author: Young-Myeong Kim

Authors: Sun-Uk Bak[1], Suji Kim[1], Hae-Jun Hwang[1], Jung-A Yun[1], Wan-Sung Kim[1], Moo-Ho Won[2], Ji-Yoon Kim[3], Kwon-Soo Ha[1], Young-Guen Kwon[4], Young-Myeong Kim[1,*]

Institution: [1]Molecular and Cellular Biochemistry and [2]Neurobiology, School of Medicine, Kangwon National University,
[3]Anesthesiology and Pain Medicine, Hanyang University Hospital,
[4]Biochemistry, College of Life Science and Biotechnology, Yonsei University,

Manuscript Type: Article

Title: Heme oxygenase-1 (HO-1)/carbon monoxide (CO) axis suppresses RANKL-induced osteoclastic differentiation by inhibiting redox-sensitive NF-κB activation

Author's name: Sun-Uk Bak[1], Suji Kim[1], Hae-Jun Hwang[1], Yun Jung-A[1], Wan-Sung Kim[1], Moo-Ho Won[2], Ji-Yoon Kim[3], Kwon-Soo Ha[1], Young-Guen Kwon[4], and Young-Myeong Kim[1*]

Affiliation: Departments of [1]Molecular and Cellular Biochemistry and [2]Neurobiology, School of Medicine, Kangwon National University, Chuncheon, Gangwon-do, 200-702, South Korea. [3]Department of Anesthesiology and Pain Medicine, Hanyang University Hospital, Seoul 133-792, South Korea. [4]Department of Biochemistry, College of Life Science and Biotechnology, Yonsei University, Seoul, 120-752, South Korea.

Running Title: Regulation of osteoclastogenesis by CO

Keywords: RANKL, osteoclastogenesis, HO-1/CO, NF-κB

Corresponding Author's Information: Tel: +82-33-250-8831; Fax: +82-33-244-3286; E-mail: ymkim@kangwon.ac.kr.

ABSTRACT

Heme oxygenase (HO-1) catalyzes heme to carbon monoxide (CO), biliverdin/bilirubin, and iron. It prevents the pathogenesis of several human diseases. Here we assessed the beneficial effect of heme degradation products on osteoclastogenesis induced by receptor activator of NF-κB ligand (RANKL). Treatment of RAW264.7 cells with CORM-2 (a CO donor) and bilirubin, but not with iron, decreased RANKL-induced osteoclastogenesis, with CORM-2 having a more potent anti-osteogenic effect. CORM-2 also inhibited RANKL-induced osteoclastogenesis and osteoclastic resorption activity in marrow-derived macrophages. Treatment with hemin, a HO-1 inducer, strongly inhibited RANKL-induced osteoclastogenesis in wild-type macrophages, but not effectively in HO-$1^{+/-}$ cells. CORM-2 reduced RANKL-induced NFATc1 expression by inhibiting IKK-dependent NF-κB activation and reactive oxygen species production. These results suggest that CO has a potent inhibitory effect on RANKL-induced osteoclastogenesis by inhibiting redox-sensitive NF-κB-mediated NFATc1 expression. Our findings indicate that HO-1/CO can act as an anti-resorption agent to reduce bone loss by blocking osteoclast differentiation.

INTRODUCTION

Bone homeostasis is strictly regulated by a physiological process involving the formation and resorption of bone by osteoblast and osteoclast. Enhanced osteoclast formation (osteoclastogenesis) is an underlining mechanism of osteolytic bone diseases, including osteoporosis, rheumatoid arthritis, and bone metastatic disease. Osteoclasts are specialized multinucleated giant cells derived from mononuclear progenitors of monocytes/macrophages lineage through a differentiation process that is mainly modulated by receptor activator of nuclear factor-κB (RANKL) and macrophage colony-stimulating factor (M-CSF) (1, 2).

RANKL-induced osteoclast differentiation is mainly modulated by TNF receptor-associated factor 6 (TRAF 6)-mediated multiple pathways, including stimulation of the transcription factors nuclear factor-κB (NF-κB) through IκB kinase (IKK) activation and activator protein-1 (AP-1) complex containing c-Fos through mitogen-activated protein kinase (MAPK) (3, 4). These transcription factors ultimately activate the transcription of transcription factor nuclear factor of activated T cells-c1 (NFATc1), which upregluates osteoclast-specific gene expression such as cathepsin K (CtsK), tartrate-resistant acid phosphatase (TRAP), matrix metalloproteinase-9 (MMP-9), and calcitonin receptor (5). Therefore, inhibiting RNAKL-induced signal pathway or osteoclast differentiation might be a potential strategy to treat bone diseases associated with excessive osteoclastogenesis.

Heme oxygenase (HO) is a rate-limiting enzyme in the degradation of heme, resulting in the liberation of iron, biliverdin/bilirubin, and carbon monoxide (CO). Among them, CO has pleiotropic biological functions, such as vasorelaxation, neurotransmission, antioxidation, anti-inflammation, and anti-apoptosis (6). Other heme catabolites biliverdin, bilirubin, and iron also have several biological activities similar to those exerted by CO (6, 7). Although some studies have proposed that CO can regulate RANKL-induced osteoclastogenesis (8-10), its underlying mechanism has not been clearly elucidated. In addition, the regulatory effects

of other heme catabolites on osteoblast differentiation have not been studied yet.

In the present study, we examined the effects of heme degradation products on RANKL-induced osteoclast differentiation and its underlying mechanism in RAW264.7 cells and mouse marrow-derived monocytes/macrophages cells (BMMs). Our results showed that CO and bilirubin, but not iron, could inhibit RANKL-induced osteoclastogenesis, with CO having more potent anti-osteogenic effect than bilirubin through inhibiting redox-sensitive NF-κB-dependent NFATc1 expression. These results suggest that the HO-1/CO pathway has a potential role in preventing bone disease associated with excessive osteoclast activity

RESULTS

Effects of CO, iron, and bilirubin on RANKL-induced osteoclastogenesis

To examine the effects of the heme degradation products, CO, iron (Fe^{2+}), and bilirubin, on osteoblast differentiation, we examined the effects of the heme catabolites on RANKL-induced osteoclastogenesis. Briefly, murine macrophage RAW264.7 cells were pretreated with or without 50 μM CORM-2 (a CO-releasing compound), iron or bilirubin for 1 h, followed by co-stimulation with RANKL (100 ng/ml) for 5 days. CORM-2 effectively inhibited RANKL-induced increase in TRAP-positive multinucleated cells, a typical marker of osteoclastogenesis (Fig. 1A and B). Bilirubin also partially suppressed osteoclast differentiation compared with the control RANKL alone; however, iron failed to significantly affect RANK-induced osteoclastogenic effects (Fig. 1A and B). The inhibitory effect of CORM-2 was dose-dependent, whereas $RuCl_3$, a control compound, failed to affect RANK-induced osteoclastogenesis (Fig. 1C and D). These results suggest that CO could potentially inhibit RANKL-induced osteoclastogenesis in immortalized macrophage RAW264.7 cells. Next, we examined the effect of CORM-2 on osteoclastogenesis in primary cultured mouse

macrophages. Treatment with CORM-2 also effectively abrogated RANKL-induced increases in osteoclastogenesis of BMMs in a concentration-dependent manner (Fig. 1E and F). We further investigated whether CO would regulate the bone resorption ability of BMMs stimulated with RANKL. When stimulated with RANKL on calcium phosphate-coated plates, BMMs increased a number of pits as a result of calcium resorption by functionally active osteoclasts differentiated from RANKL-treated BMMs, and the pit formation was inhibited by CORM-2 in a concentration-dependent manner (Fig. 1G and H). These results suggest that CO inhibits RANKL-induced osteoclast differentiation and bone resorption.

CO suppresses RANKL-induced osteoclast marker gene expression

RANKL induces osteoclast differentiation by increasing the expression levels of NFATc1 and the AP-1 component c-Fos, which stimulate the expression of osteoblast-specific genes (4). As expected, RANKL significantly increased the expression level of NFATc1, but not c-Fos, based on qRT-PCR and Western blot analyses. Such increase was abrogated by treatment with CORM-2 (Figure 2A and B). Furthermore, CORM-2 significantly decreased the protein levels of NFATc1, but not c-Fos, in the nuclear fraction (Fig. 2C). Under the same experimental conditions, NFATc1-dependent osteoblast marker genes, such as TRAP, Ctsk, and OSCAR, were induced in response to RANKL, and these increases were significantly blocked by CORM-2 (Fig. 2D-F). These data indicate that CO can suppress osteoblast-specific marker gene expression by inhibiting RANKL-induced expression of NFATc1.

Heme-mediated HO-1 induction suppresses RANKL-induced osteoclastogenesis

To examine whether endogenous CO could regulate RANKL-induced osteoclastogenesis, BMMs were treated with hemin (a substrate and potent inducer of HO-1) to elicit HO-1 induction, followed by stimulation with RANKL in the presence of M-CSF for 5 days. When

treated with hemin, HO-1 was strongly induced in BMMs from wild-type mice, but weakly expressed in cells from HO-$1^{+/-}$ mice (Fig. 3A). Hemin treatment strongly inhibited RANKL-induced osteoclastogenesis in BMMs from wild-type, but not effectively in cells from HO-$1^{+/-}$ mice, and these inhibitions were reversed by the HO-1 inhibitor SnPP (Fig. 3B and C). These results suggest that HO-1-derived CO may play an important role in negative regulation of osteoclastogenesis.

CO inhibits RANKL-induced activation of NF-κB, but not MAPKs or Akt

During osteoclast differentiation, NFATc1 expression depends on the activation of transcription factors, such as AP-1 and NF-κB, by stimulating MAPKs and IκB degradation, respectively (4, 5). We examined the effects of CO on RANKL-induced activation of MAPKs. RANKL increased phosphorylation-dependent activation of ERK, JNK, and p38, and these activations were not significantly affected by CORM-2 treatment (Fig. 4A). Next, we examined the effects of CO on RANKL-induced NF-κB activation via IκB degradation elicited by activating IKK, NIK, and Akt (11). RANKL increased phosphorylation of IKKα/β (Ser180/181) and Akt, but not NIK (Fig. 4B). CORM-2 treatment inhibited RANKL-induced phosphorylation of IKKα/β, but not Akt, resulting in the suppression of RNAKL-mediated IκBα (Ser32) phosphorylation and degradation (Fig. 4B). As a result, CORM-2 blocked RNAKL-induced nuclear translocation of the NF-κB p65 subunit (Fig. 4C and D). Inhibition of the NF-κB pathway by CORM-2 was highly correlated with its suppressive effect on RANKL-induced reactive oxygen species (ROS) production (Fig. 4E), suggesting that CO could inhibit RANKL-induced redox-sensitive NF-κB activation. Moreover, CORM-2 abrogated RNAKL-induced NF-κB reporter activity (Fig. 4F). We further examined whether CORM-2 could regulate NF-κB binding to the κB element at -664 bp upstream in the murine

NFATc1 promoter (5). Chromatin immunoprecipitation (ChIP) analysis showed that CORM-2 significantly decreased RANKL-induced binding of NF-κB to NFATc1 promoter (Fig. 4G). In addition, CORM-2 inhibited RNAKL-induced transcriptional activity of NFATc1 promoter (Fig. 4H). These results indicate that CO inhibits RANKL-induced NF-κB signal pathway by inhibiting IKK activation, resulting in the inhibition of NFATc1 expression.

DISCUSSION

This study was undertaken to elucidate the potential inhibitory effect and molecular mechanism of heme catabolites on RANKL-induced osteoclastic differentiation, a key process in bone metabolism. Here we found that exogenous CO (generated by CORM-2) and bilirubin, but not iron, suppressed RANKL-induced osteoclastogenesis or osteoclastic resorption activity in RAW264.7 cells and BMMs, with CO having a more potent effect than bilirubin. Similar anti-osteoclastogenic effect was observed in wild-type BMMs treated with hemin, a HO-1 inducer; however, the effect of hemin was much less in HO-$1^{+/-}$ cells. The anti-osteoclastogenic activity of CO was associated with inhibition of redox-sensitive NF-κB-dependent NFATc1 expression, leading to the suppression of NFATc1-mediated expression of osteoclast-specific genes. These results suggest that the HO-1/CO axis can potentially restrains osteoclastogenesis and prevent bone loss by inhibiting NF-κB-dependent NFATc1 expression.

HO-1 is recognized as a cytoprotective, antioxidant, and anti-inflammatory gene by catabolizing heme to biliverdin (finally converts to bilirubin), iron, and CO (7). Among these products, CO plays the most important role in HO-1-mediated biological function (12). Other metabolites also have similar biological activity through ROS scavenging or induction of the antioxidant gene ferritin (7, 12). Indeed, it has been demonstrated that exogenous CO gas or

CO-releasing molecules have beneficial effect as therapeutic treatment in animal models of inflammatory diseases and traumatic brain injury (13, 14). Moreover, a number of studies have shown that HO-1 expression or CO delivery can prevent inflammatory arthritis and bone loss in animal models (8-10) probably by suppressing either inflammatory cytokine production or osteoclast differentiation. Similarly, we found that induction of HO-1 or treatment with CORM-2 or bilirubin, but not iron, prevented RANKL-induced osteoclast differentiation, with bilirubin having less anti-osteoclastogenic activity compared to CO. This indicates that, among HO-1 metabolites, CO is a major contributor to the preventive effect of HO-1 on osteoblast differentiation.

RANKL induces osteoclast differentiation from BMMs by triggering the intracellular signal pathway that promote induction or activation of transcription factors, such as NFATc1 and NF-κB (4, 5). NFATc1 is a key transcription factor for osteoclast differentiation, because Nfatc1$^{-/-}$ embryonic stem cells cannot differentiate into osteoclasts *in vitro* and overexpression of NFATc1 induces osteoclastogenesis (15). It is evident that NFATc1 is transcriptionally induced and acts as a master transcription factor for RANKL-induced osteoblast differentiation. NFATc1 is robustly induced through an autoamplification circuit by binding to its own promoter (5). NFATc1 promoter also cooperatively interacts with other RNAKL-stimulated transcription factors, such as NF-κB and AP-1 to activate the initial induction of NFATc1, followed by an autoamplification phase of NFATc1, indicating that activation of NF-κB and AP-1 plays an important role in RANKL-induced osteoclastogenesis (5). Herein, we found that CO inhibited RANKL-induced NFATc1 expression by suppressing IKK-dependent NF-κB activation, but not the AP-1 component c-Fos expression, leading to the suppression of NFATc1-targeted osteoclast marker genes, including TRAP, Ctsk, and OSCA. On the other hand, RANKL also activates MAP kinase (MAPK) and Akt to induce

the expression of critical genes for osteoclast differentiation (4). In general, NF-κB is activated by several upstream signal mediators, such as IKK, Akt, and MAPKs (16). However, our data showed that CO only inhibited IKK, not others, which were activated by RANKL. More interestingly, CORM inhibited RANKL-induced ROS generation, an upstream of IKK (16), suggesting that CO dampens ROS-dependent IKK activation. These results suggest that CO inhibits RANKL-mediated NFATc1 autoamplification and osteoclastogenesis through initial suppression of the ROS/IKK/NF-κB pathway, but not other signal mediators.

CO inhibits NF-κB activation in response to inflammatory stimuli, including lipopolysaccharide and TNF-α, resulting in the prevention of inflammatory diseases. Several mechanisms have been proposed to explain the inhibitory effect of CO-mediated NF-κB activation. First, CO inhibits the redox-sensitive NF-κB signaling pathway by decreasing ROS production via inhibition of NADPH oxidase activation in response to LPS or TNF-α (17, 18). Interestingly, RANKL increases NADPH oxidase-dependent ROS production, which stimulates osteoblast differentiation by activating NF-κB (19, 20). Consistent with previous evidence showing that CO and bilirubin have potent antioxidant activity (7, 21), we found that CORM-2 inhibited RANKL-induced ROS generation. Thus, it is possible that CO inhibits RANKL-mediated NADPH oxidase activation and ROS accumulation, resulting in inhibition of redox-sensitive IKK-mediated NF-κB activation. The anti-osteogenic effect shown by bilirubin might be associated with the inhibition of NF-κB activation via its antioxidant activity which inhibits ROS generation and IKK activation (19, 20), although these evidence has not been provided. Another possibility is associated with S-glutathiolation of the NF-κB p65 subunit, which is independent of IKK activation (22). Our data showed that CO inhibited IKK-dependent IκBα phosphorylation and degradation, indicating that CO

might not be able to stimulate S-glutathiolation of p65 in macrophages stimulated with RANKL.

Taken together, our data demonstrated that CO could inhibit RANKL-induced osteoclastogenesis by suppressing NF-κB-dependent NFATc1 expression, probably by dampening ROS production. Our results provide new insight into therapeutic potential of CO for treating abnormal bone metabolism and osteolytic bone diseases.

MATERIALS AND METHODS

Materials

Dulbecco's modified Eagle's medium (DMEM), α-minimum essential medium (α-MEM), and supplements were purchased from Invitrogen Life Technologies (Carlsbad, CA), and fetal bovine serum (FBS) was obtained from HyClone Laboratories (Logan, UT). Recombinant murine sRANKL and macrophage-colony stimulating factor (M-CSF) were purchased from PeproTech (Rock Hill, NJ, USA). Tricarbonyldichlororuthenium (II) dimer (CORM-2), bilirubin, $FeCl_2$, and ruthenium chloride ($RuCl_3$) were purchased from Sigma-Aldrich (St Louis, MO, USA). All antibodies used in this study were purchased from Santa Cruz (Santa Cruz, CA, USA) or Cell Signaling (Beverly, MA, USA). Anti-NFATc1 monoclonal antibody was purchased from BD Biosciences Discovery Lab-ware (Bedford, MA).

Cell culture

Murine macrophage cell line RAW264.7 cells (2.5 x 10^3 cells/well in 96 well plate) were cultured in DMEM supplemented with 10% FBS, 100 units/ml penicillin, and 100 units/ml streptomycin. Bone marrow cells were collected from the tibia and femur of 6 week-old female C57BL/6 mice. The bone marrow suspension was cultured in α-MEM containing

10% FBS for 24 h. Nonadherent cells were collected and cultured with and 5 ng/ml of M-CSF in a 96-well plates at 5 x10^6 cells/well. After 2 days, nonadherent cells including lymphocytes were washed out, and adherent cells were used as BMMs.

Osteoclast differentiation and TRAP staining

After pretreatment with the indicated concentrations or 50 μM of CORM-2 and $RuCl_3$ for 1 h, BMMs were cultured with 100 ng/ml RANKL and 10 ng/ml M-CSF, and RAW264.7 cells were stimulated with or without 100 ng/ml RANKL. After 3 days, the culture media were replaced with fresh complete media containing the same concentrations of RANKL, CORM-2, and $RuCl_3$. After another 2 days, cells were fixed with 3.7% formaldehyde for 5 min at room temperature, washed twice with phosphate-buffed saline (PBS), and stained to visualize TRAP using a leukocyte acid phosphatase kit (Sigma-Aldrich, St Louis, MO, USA). TRAP-positive multinucleated cells (more than 3 nuclei) were counted as osteoclasts using optical microscopy.

Pit formation assay

BMMs were seeded at a density of 6 x 10^4 cells/well in 96-well calcium-phosphate-coated OAAS™ plates and stimulated with 10 ng/ml M-CSF and 100 ng/ml RANKL in presence of different concentrations of CORM-2. After 7 days, the medium was removed to measure the resorption area of calcium-phosphate, and the cells were gently detached by treating plates with 5% sodium hypochlorite for 5 min. The resorption areas were captured using a microscope and analyzed by image-analyzing software, Image proplus™.

Quantative reverse transcription-polymerase chain reaction (qRT-PCR)

Total RNAs were isolated using the Trizol reagent kit (Life Technology Inc., USA). Five μg of mRNA was converted to cDNA by treatment with 200 units of reverse transcriptase and 500 ng of oligo-dT_{18} primer in 50 mM Tris-HCl (pH 8.3), 75 mM KCl, 3 mM $MgCl_2$, 10 mM DTT, and 1 mM dNTPs at 42°C for 1 h. The reaction was stopped by heating at 70°C for 15 min and 1 μl of cDNA mixture was used for enzymatic amplification. qRT-PCR analysis was performed using a Roter-Gene Q real-time PCR cycler (Qiagene). The expression of target molecules was analyzed using SYBR Green-based qRT-PCR, and normalized to the expression of *GAPDH*. The specific primer sets were as follows: *NFATc1*, 5′-GAGTACACCTTCCAGCACCTT-3′ (sense) and 5′-TATGATGTCGGGGAAAGAGA-3′ (antisense); *TRAP*, 5′-TCATGGGTGGTGCTGCT-3′ (sense) and 5′-GCCCACAGCCACAAATCT-3′ (antisense); *OSCAR*, 5′-GGAATGGTCCTCATCTCCTT-3′ (sense) and 5′-TCCAGGCAGTCTCTTCAGTTT-3′ (antisense); *CtsK*, 5′-CCAGTGGGAGCTATGGAAGA-3′ (sense) and 5′-CTCCAGGTTATGGGCAGAGA-3′ (antisense); *GAPDH*, 5′-TCAAGAAGGTGGTGAAGCAG-3′ (sense) and 5′-AGTGGGAGTTGCTGTTGAAGT-3′ (antisense).

Localization of the NF-κB p65 subunit

Cells were cultured on glass slides and stimulated with 100 ng/ml RANKL in the presence or absence of CORM-3. Cells were fixed with 3.7% formaldehyde in PBS for 15 min at 4°C, washed with PBS, and permeabilized with 0.1% saponin for 30 min at 4°C. The slides were incubated with goat polyclonal anti-p65 antibody (1:50, Santa Cruz Biotechnology). After 2 h, the cells were washed with PBS and incubated with anti-goat IgG-FITC (1:100, Sigma) for 1 h and were further incubated for 30 min with DAPI (1 μg/ml, Sigma) for nuclear staining. The cells were mounted with mounting medium and observed by laser scanning confocal microscopy (Olympus).

Other biochemical analyses

Whole cell lysates, cytosolic fractions, and nuclear extracts were prepared as previously described (23). After protein concentration was measured by a BCA method, samples (30 mg protein) were electrophoresed on a 10% SDS-PAGE and target protein levels were determined by Western blot analysis. Intracellular ROS accumulation was determined RAW264.7 cells stimulated with 100 ng/ml RANKL in the presence or absence of CORM-2 for 20 min, as previously described (24) using DCFH-DA. ChIP assay was performed using cells stimulated with RANKL (100 ng/ml) in the presence or absence of CORM-2 (50 μM) for 2 h as described in the manufacturer's instructions of Millipore ChIP Assay Kit (Millipore, Temecula, CA). Target sequences of NFATc1 promoter sequences were identified by PCR (30 cycles at 94°C for 1 min, 52°C for 1 min, 72°C for 30 s) using primer pairs spanning NFATc1-specific promoter regions containing NF-κB-binding sequence, forward 5'-ACGCCCATGCAATCTGTTAG-3' and reverse 5'-TTGCATGCTGAAGTCATTATGT-3', which amplify a 130 bp product. Products were identified on a 1.5% agarose gel. For reporter gene assay, RAW264.7 cells were transfected with 2 μg of NF-κB-Luc or NFATc1 promoter-Luc construct or each basic plasmid using Lipofectamine 3000. After 4 h incubation, cells were recovered in fresh medium for 24 h, followed by incubation with RANKL (100 ng/ml) in the presence or absence of CORM-2 for 24 h. Reporter gene activity was assayed using a luciferase assay kit.

Statistical analysis

Quantitative data are expressed as mean ± standard deviation (SD) from three independent experiments performed in triplicate. All statistical analyses were performed with GraphPad

Prism 5.0 for windows (GraphPad Software). Statistical significance was determined using one-way analysis of variance (ANOVA) or the unpaired Student's *t* test, depending on the number of experimental groups analyzed. Significance was established at a *P* value <0.05.

ACKNOWLEDGMENTS

This study is supported by 2015 Research Grant from Kangwon National University (No. 520150332) and by the National Research Foundation of Korea (NRF) Grant funded by the Korea Government (MSIP) (2013M3A9B6046563).

FIGURE LEGENDS

Fig. 1. Effects of CO, iron, and bilirubin on RANKL-induced osteoclastogenesis. (A-D) RAW264.7 cells were pretreated with the indicated concentrations or 50 μM of CORM-2 (CORM), ferrous iron or bilirubin (BR) as well as 100 μM $RuCl_3$ for 1 h, followed by co-stimulation with RANKL (100 ng/ml) for 5 days. (A and C) Cells were stained with TRAP reagent. (B and D) TRAP-positive multinucleated cells were counted through optical microscopy. (E-H) Mouse BMMs cultured on normal (E and F) or calcium-phosphate-coated plate (G and H) were treated with M-CSF and RANKL in the presence or absence of 100 μM $RuCl_3$ or 50 μM CORM-2 for 5 days. (E) Cells were stained with TRAP reagent. (F) TRAP-positive cells were counted. (G and H) Resorption pit areas were determined after 7 days and quantitated using image analyzing software (Image proplus^{TM}). *, $p < 0.05$ and **, $p < 0.01$ *versus* RANKL alone or in combination with $RuCl_3$.

Fig. 2. CO inhibits RANKL-induced NFATc1 and osteoclast marker gene expression. RAW264.7 cells were treated with RANKL (100 ng/ml) following pretreatment with CORM-2 (CORM, 50 μM). (A) After 24 h, NFATc1 and β-actin mRNA levels were determined by RT-PCR analysis and quantitated by densitometry. (B and C) After 24 h, NFATc1 and C-Fos levels in whole cell extracts and nuclear fractions were determined by Western blotting. (D-F) After 72 h, mRNA levels of TRAP, CtsK, and OSCAR were determined by RT-PCR analysis and quantitated by densitometry. *, $p < 0.05$ and **, $p < 0.01$ *versus* RANKL alone.

Fig. 3. Hemin-induced HO-1 inhibits RANKL-mediated osteoclastogenesis. (A-C**)** BMMs isolated wild-type (WT) and HO-$1^{+/-}$ mice were treated with hemin (2 μM) for 8 h (A), followed by stimulation with M-CSF and RANKL in the presence or absence of SnPP (1 μM)

for 5 days. (A) HO-1 levels were determined by Western blotting. (B and C) TRAP-positive multinucleated cells were counted through optical microscopy.

Fig. 4. CO inhibits RANKL-induced activation of NF-κB, but not MAPKs or Akt. RAW264.7 cells were treated with RNAKL (100 ng/ml) alone or in combination with CORM-2 (CORM, 50 μM). (A and B) After 30 min, phosphorylated levels of MAPKs (A) and NF-κB signal mediators (B) were determined by Western blotting. (C) After 1 h, NF-κB p65 levels were determined in the cytosolic and nuclear fractions by Western blotting. (D) Nuclear translocalization of p65 was determined by confocal laser microscopy. (E) After 20 min, intracellular ROS levels were determined by confocal microscopy using DCF-DA. (F) Cells were transfected with a NF-κB-Luc construct, followed by treatment with RANKL alone or in combination with CORM-2 for 24 h. Luciferase activity was determined in cell lysates. (G) NF-κB binding to NFATc1 promoter was determined by ChIP analysis. (H) NFATc1 promoter activity was determined by luciferase-reporter gene expression assay. *, $p < 0.05$ *versus* RANKL alone.

REFERENCES

1. Asagiri M and Takayanagi H (2007) The molecular understanding of osteoclast differentiation. Bone 40, 251– 264
2. Boyle WJ, Simonet WS and Lacey DL (2003) Osteoclast differentiation and activation. Nature 423, 337– 342
3. Kobayashi N, Kadono Y, Naito A et al (2001) Segregation of TRAF6-mediated signalling pathways clarifies its role in osteoclastogenesis. EMBO J 20, 1271-1280
4. Walsh MC, Kim N, Kadono Y et al (2006) Osteoimmunology: interplay between the immune system and bone metabolism. Annu Rev Immunol 24, 33-63
5. Asagiri M, Sato K, Usami T, Ochi S, Nishina H and Yoshida H (2005) Autoamplification of NFATc1 expression determines its essential role in bone homeostasis. J Exp Med 202, 1261– 1269
6. Ayer A, Zarjou A, Agarwal A and Stocker R (2016) Heme oxygenases in cardiovascular health and disease. Physiol Rev 96, 1449-1508
7. Kim YM, Pae HO, Park JE et al (2011) Heme oxygenase in the regulation of vascular biology: from molecular mechanisms to therapeutic opportunities. Antioxid Redox Signal 14, 137-167
8. Van Phan T, Sul OJ, Ke K et al (2013) Carbon monoxide protects against ovariectomy-induced bone loss by inhibiting osteoclastogenesis. Biochem Pharmacol 85, 1145-1152
9. Tseng FJ, Chia WT, Wang CH et al (2015) Carbon monoxide inhibits receptor activator of NF-κB (RANKL)-induced osteoclastogenesis. Cell Physiol Biochem 36, 1250-1258
10. Ke K, Safder MA, Sul OJ et al (2015) Hemeoxygenase-1 maintains bone mass via attenuating a redox imbalance in osteoclast. Mol Cell Endocrinol 409, 11-20
11. Boyce BF (2013) Advances in the regulation of osteoclasts and osteoclast functions. J Dent Res 92, 860-867

12. Ryter SW, Alam J and Choi AM (2006) Heme oxygenase-1/carbon monoxide: from basic science to therapeutic applications. Physiol Rev 86, 583-650

13. Lee S, Lee SJ, Coronata AA et al (2014) Carbon monoxide confers protection in sepsis by enhancing beclin 1-dependent autophagy and phagocytosis. Antioxid Redox Signal 20, 432-442

14. Choi YK, Maki T, Mandeville ET et al (2016) Dual effects of carbon monoxide on pericytes and neurogenesis in traumatic brain injury. Nat Med 22, 1335-1341

15. Takayanagi H, Kim S, Koga T et al (2002) Induction and activation of the transcription factor NFATc1 (NFAT2) integrate RANKL signaling in terminal differentiation of osteoclasts. Dev Cell 3, 889-901

16. Santoro MG, Rossi A and Amici C (2003) NF-κB and virus infection: who controls whom. EMBO J 22, 2552-2560

17. Nakahira K, Kim HP, Geng XH et al (2006) Carbon monoxide differentially inhibits TLR signaling pathways by regulating ROS-induced trafficking of TLRs to lipid rafts. J Exp Med 203, 2377-2389

18. Chi PL, Liu CJ, Lee IT, Chen YW, Hsiao LD and Yang CM (2014) HO-1 induction by CO-RM2 attenuates TNF-α-induced cytosolic phospholipase A2 expression via inhibition of PKCα-dependent NADPH oxidase/ROS and NF-κB. Mediators Inflamm 2014, 279171

19. Lee NK, Choi YG, Baik JY et al (2005) A crucial role for reactive oxygen species in RANKL-induced osteoclast differentiation. Blood 106, 852-859

20. Ha H, Kwak HB, Lee SW et al (2004) Reactive oxygen species mediate RANK signaling in osteoclasts. Exp Cell Res 301, 119-127

21. Stocker R, Yamamoto Y, McDonagh AF, Glazer AN and Ames BN (1987) Bilirubin is an

antioxidant of possible physiological importance. Science 235, 1043-1046

22. Yeh PY, Li CY, Hsieh CW, Yang YC, Yang PM and Wung BS (2014) CO-releasing molecules and increased heme oxygenase-1 induce protein S-glutathionylation to modulate NF-κB activity in endothelial cells. Free Radic Biol Med 70, 1-13
23. Kang N, Koo J, Wang S, Hur SJ and Bahk YY (2016) A systematic study of nuclear interactome of C-terminal domain small phosphatase-like 2 using inducible expression system and shotgun proteomics. BMB Rep 49, 319-324
24. Park GS, Kim JK and Kim JH (2016) Anti-inflammatory action of ethanolic extract of Ramulus mori on the BLT2-linked cascade. BMB Rep 49, 232-237

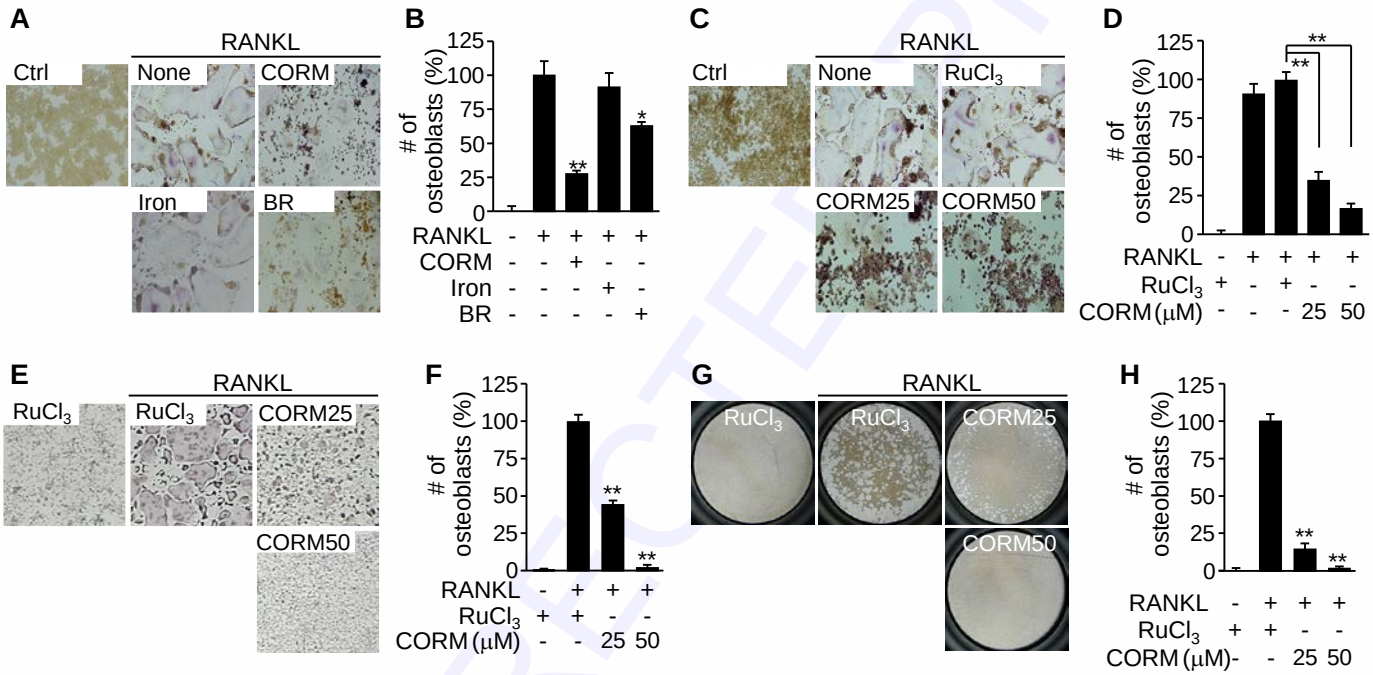

Figure 1

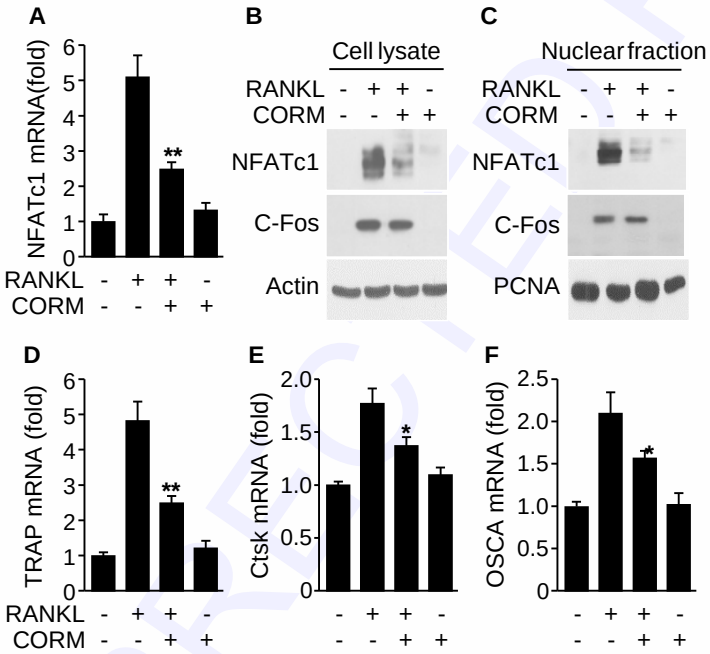

Figure 2

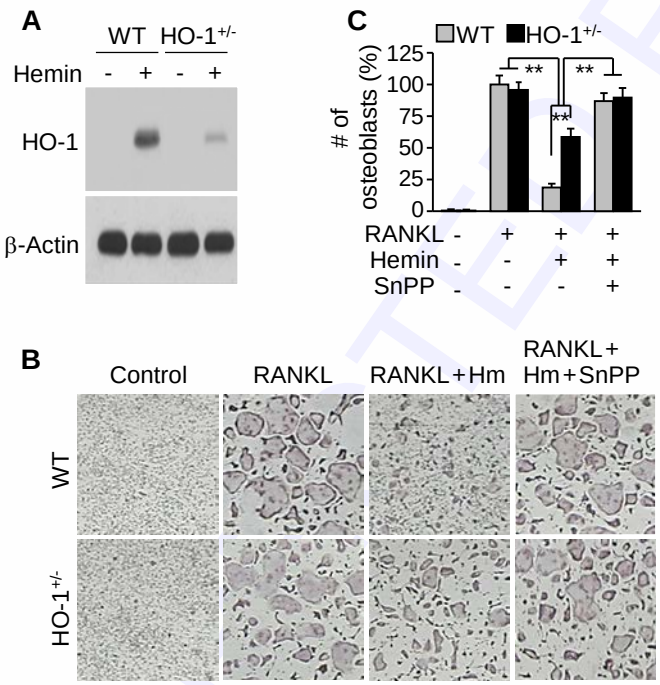

Figure 3

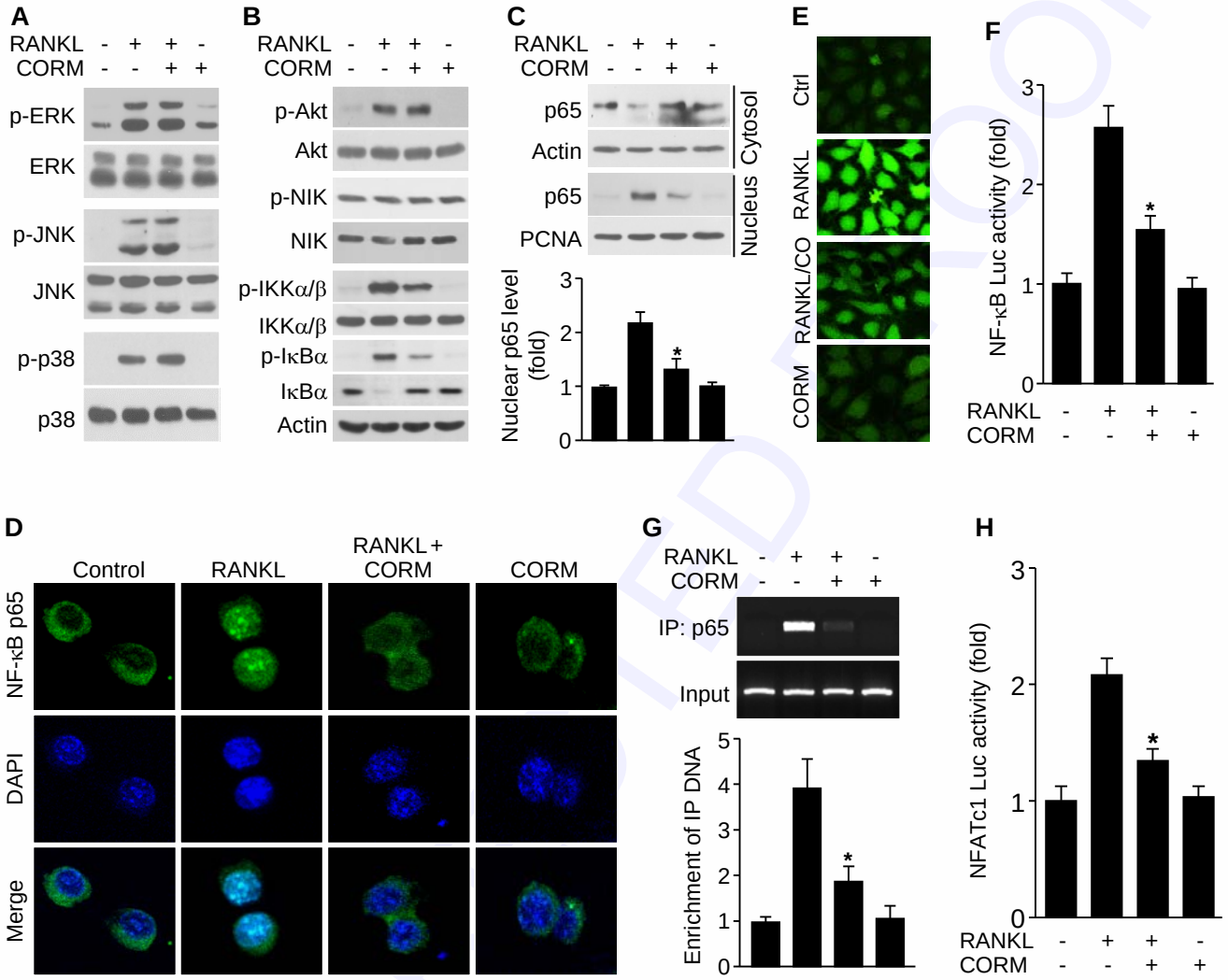

Figure 4